BIRA-IASB aeronomie.be

Comparing ground-based remote sensing measurements to in situ measurements at Jungfraujoch

ACTRiS

EMPA

LIÈGE université

B. Dils, M. Zhou, F. Hendrick, J. Cui, B. Franco, D. Helmig, S. Henne, C.Hoerger, J. Hueber, E.Mahieu, A. Merlaux, J.-F. Müller, S. Reimann, T. Seitz, M. Steinbacher, T. Stavrakou, R.Sussmann, M. Van Roozendael, and M. De Mazière

Introduction

• A bit of history

- First measurements in 1950/1951 with a grating spectrometer
- Mid-70'ies return with an improved grating spectrometer
- Mid 80'ies FTIR

- Network for detection of stratospheric Change (NDSC)

- Unique 60000+ spectra, multi-decade dataset operated by the GRIPAS team at Liège University

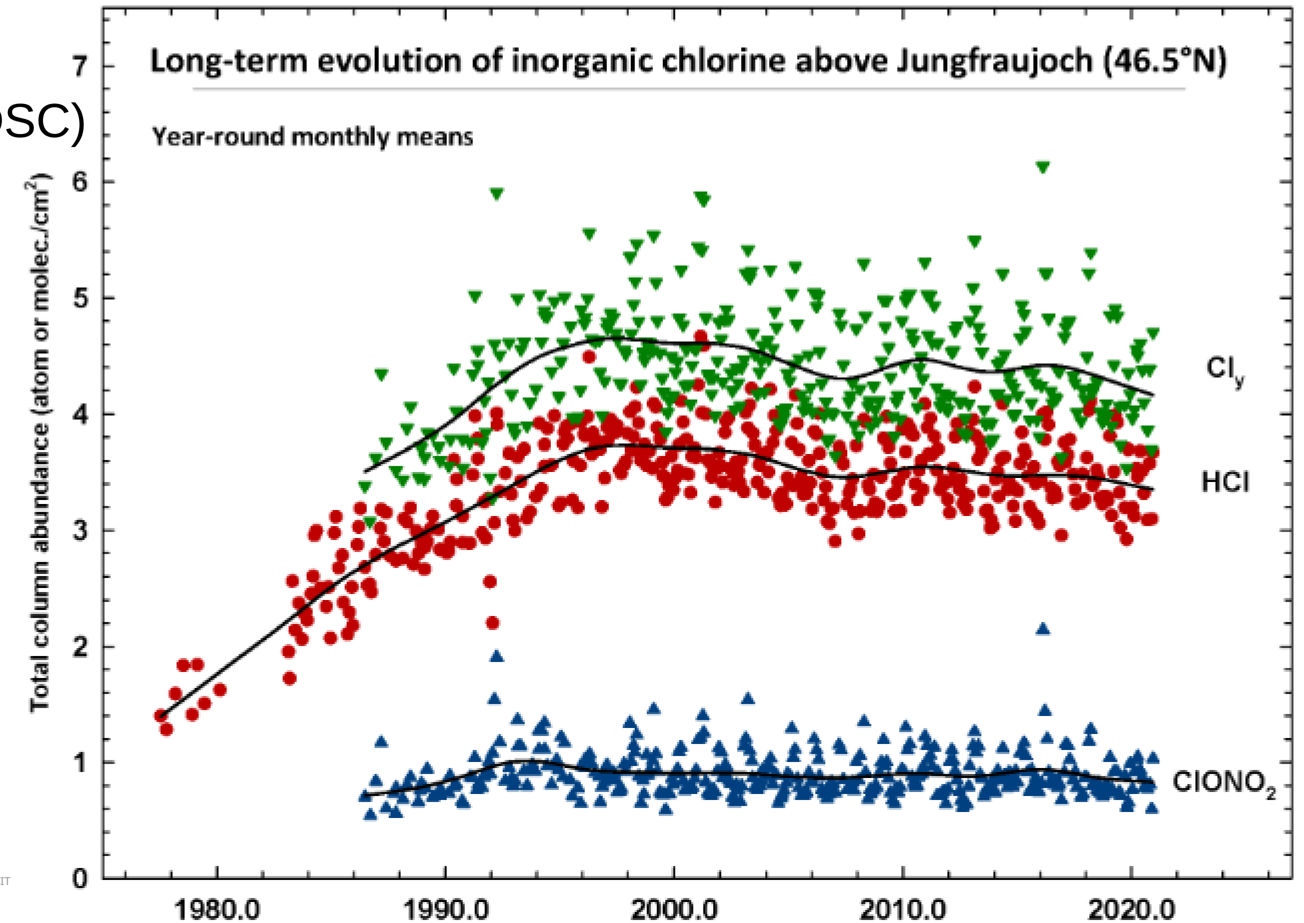

Mahieu, E., Bader, W., Bovy, B., et al.: Surveillance de l'atmosphère terrestre depuis la station du Jungfraujoch :
une épopée liégeoise entamée voici plus de 65 ans !, Bull. de la Société Géographique Liège, 68, 119–130, 20

KYOTO-PROTOCOL RELATED MEASUREMENTS AT THE JUNGFRAUJOCH

NDSC → NDACC

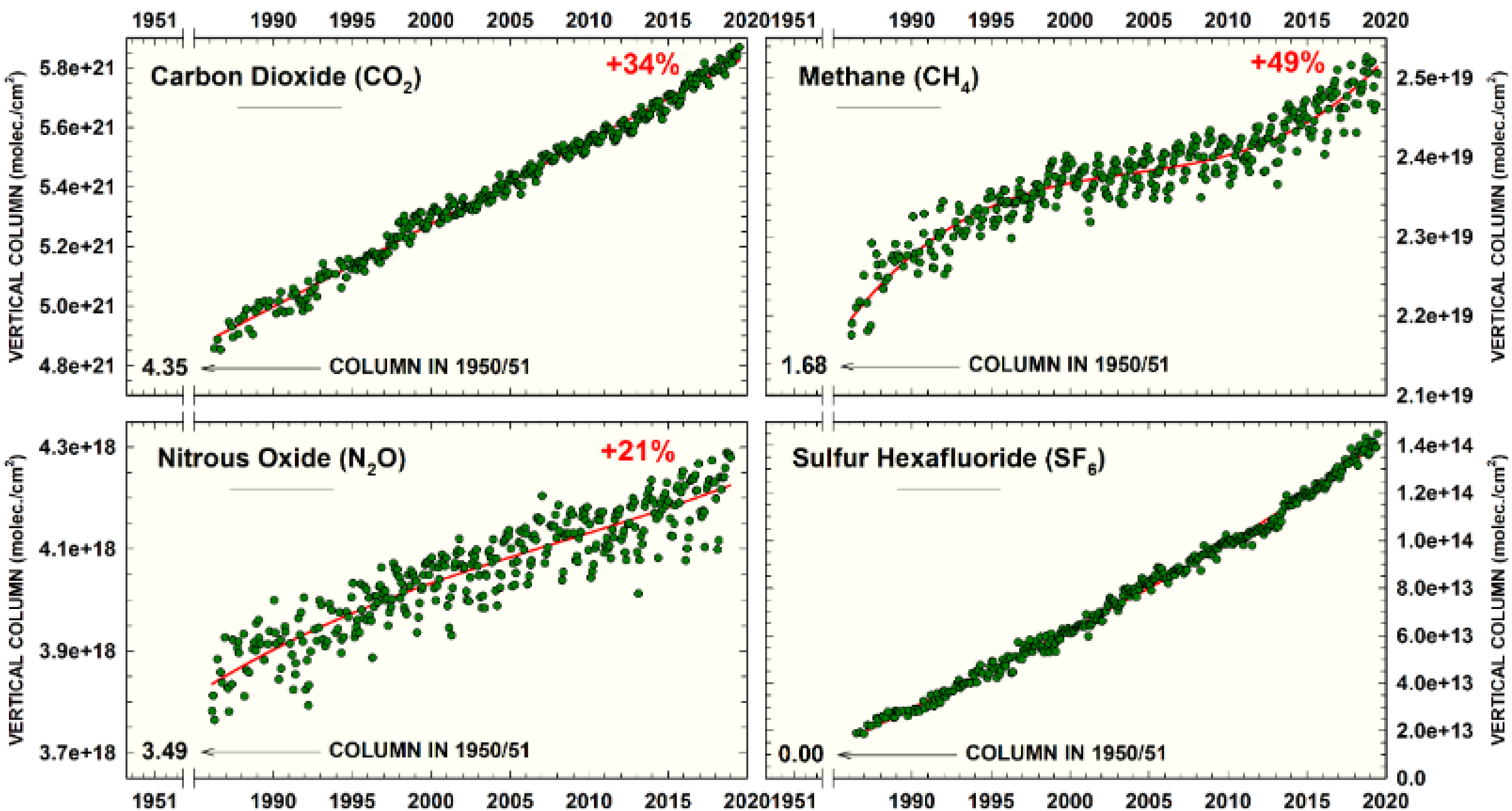

List of species monitored by FTIR remote-sensing at the Jungfraujoch station		
Greenhouse gases	H_2O, CO_2, CH_4, N_2O, CF_4, SF_6	Support to the Kyoto Protocol and the Paris Agreement
Ozone-related	O_3, NO, NO_2, $ClONO_2$, HCl, HF, COF_2, CFC-11, -12, HCFC-22, -142b, CCl_4, CH_3Cl	Support to the Montreal Protocol
Air quality, biomass burning, oil & gas sector	CO, CH_3OH, C_2H_6, C_2H_2, C_2H_4, HCN, HCOOH, HCHO, NH_3, PAN	Support to the Copernicus CAMS program of EU
Others	OCS, N_2, isotopologues	Various applications

- Zenith-sky DOAS since 1991 → optimized for stratospheric NO2 and O3
- MAX-DOAS: end 2010 – mid 2016
  - Slant column measurements of lower troposphere
  - HCHO, NO2, aerosols

• FTIR and DOAS configuration

- FTIR uses direct sun IR radiation (can only operate under clear sky conditions)
- DOAS Measures the absorption of sunlight scattered by molecules and aerosols in the UV-visible range
- Off-axis viewing directions + zenith:
- Both methods use an Optimal estimation approach (but differ greatly in terms of vertical sensitivity and resolution) ⟶ Averaging Kernel

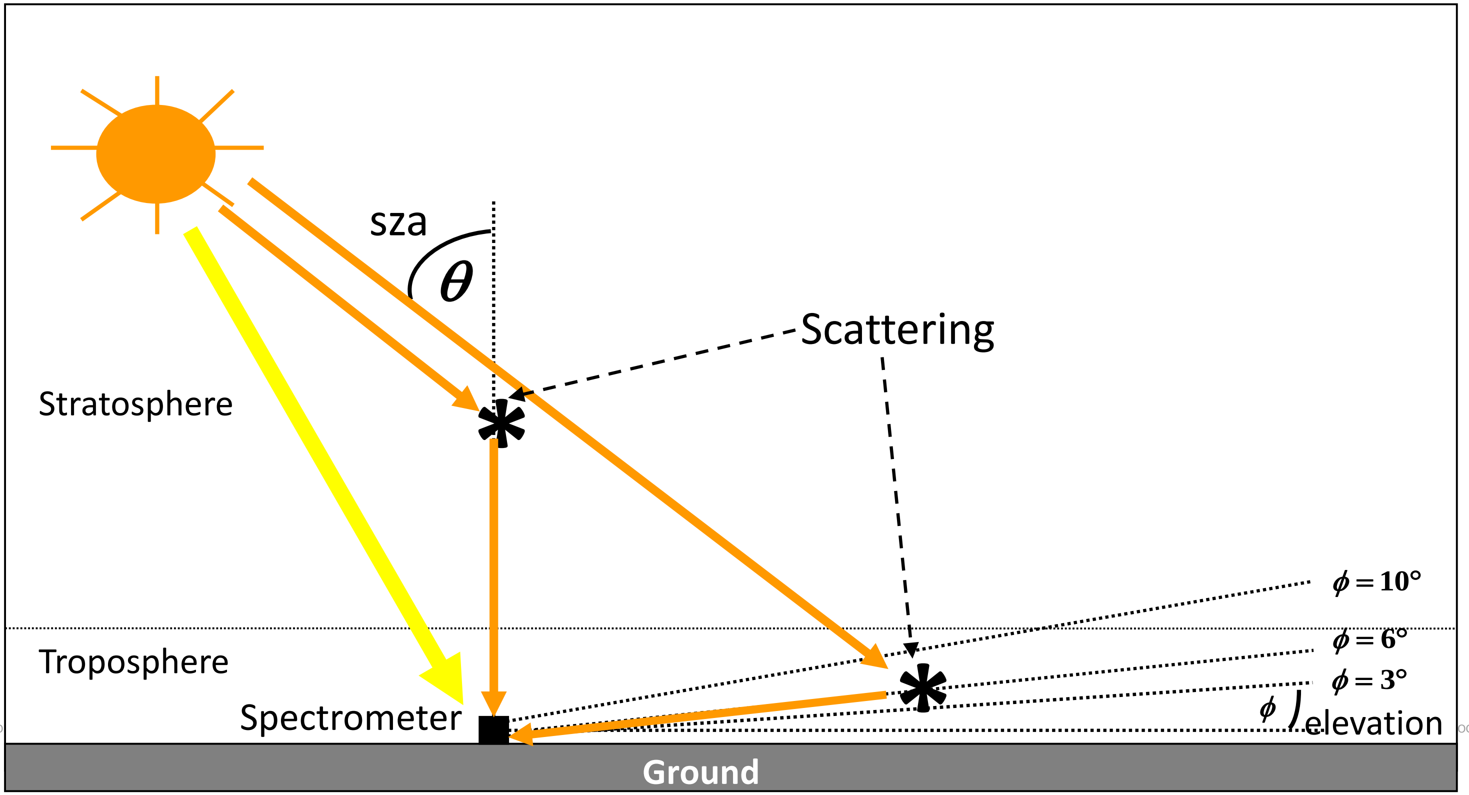

Uncertainties

uncertainties

- GEOMS (=FTIR/DOAS reporting data format) uses variable "descriptors" to provide information on the uncertainties for a variable

- CO.MIXING.RATIO.VOLUME.DRY_ABSORPTION.SOLAR_<u>UNCERTAINTY.RANDOM.COVARIANCE</u>

- descriptors used in the data files are

```
=UNCERTAINTY.RANDOM.STANDARD;
=UNCERTAINTY.RANDOM.STANDARD.RELATIVE;
=UNCERTAINTY.RANDOM.COVARIANCE;


=UNCERTAINTY.SYSTEMATIC.STANDARD;
=UNCERTAINTY.SYSTEMATIC.STANDARD.RELATIVE;
=UNCERTAINTY.SYSTEMATIC.COVARIANCE;
```

- random=uncorrelated noise (in time) systematic=correlated (in time) … related to "mean bias"

- profiles are reported with 2D covariance matrices (contains "correlation" information in the vertical axis) so that uncertainties on partial columns can be derived (tropospheric/stratospheric columns eg)

Uncertainty estimation

- profiles are obtained from Optimal Estimation and the uncertainty analysis in Rodgers 2000 is used:

$$\begin{aligned} \hat{\mathbf{x}} - \mathbf{x} \;=\; & (\mathbf{A} - \mathbf{I}_n)(\mathbf{x} - \mathbf{x}_a) && \ldots \textit{smoothing error} \\ & + \mathbf{G}_y \mathbf{K}_b (\mathbf{b} - \hat{\mathbf{b}}) && \ldots \textit{model parameter error} \\ & + \mathbf{G}_y \Delta \mathbf{f}(\mathbf{x}, \mathbf{b}, \mathbf{b}') && \ldots \textit{forward model error} \\ & + \mathbf{G}_y \boldsymbol{\epsilon} && \ldots \textit{retrieval noise} \end{aligned} \quad (3.16)$$

- An estimate of the random/systematic uncertainty of each input parameter is determined and propagated to the retrieved profile: eg spectroscopy, temperature, h2o, solar zenith angle, spectral noise, … ~~prior/smoothing error~~

- The final uncertainties are summed uncertainties of the propagated input parameters

Uncertainty estimation

$$
\begin{aligned}
\hat{\mathbf{x}} - \mathbf{x} \quad = \quad & (\mathbf{A} - \mathbf{I}_n)(\mathbf{x} - \mathbf{x}_a) && \textit{...smoothing error} \\
& + \mathbf{G}_y \mathbf{K}_b (\mathbf{b} - \hat{\mathbf{b}}) && \textit{...model parameter error} \\
& + \mathbf{G}_y \Delta \mathbf{f}(\mathbf{x}, \mathbf{b}, \mathbf{b}') && \textit{...forward model error} \\
& + \mathbf{G}_y \epsilon && \textit{...retrieval noise}
\end{aligned}
\qquad (3.16)
$$

- Some examples of the estimation of the model paramater uncertainties
  - spectroscopic uncertainties from HITRAN or educated guess
  - other uncertainty estimates: from comparisons with independent measurements, eg NCEP temperature is compared to sonde temperature profiles

a rough estimate on T uncertainty is derived, eg
random: 2K->4K->2K in tropo, 5K>30km
systematic: .2K<10km, 3K between 10km and 15km, 1K>15km

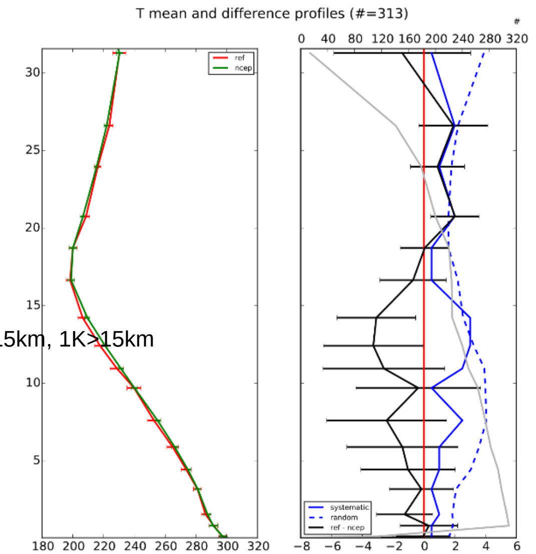

Uncertainty budget/Information content/vertical sensitivity

Table 2. Impact of major sources of systematic and random uncertainties on typical individual HCHO total column retrievals from FTIR solar spectra above the Jungfraujoch station. These uncertainties have been calculated on the basis of all individual solar spectra recorded during the year 2011 with the exception of the measurement noise, smoothing and model parameter contributions that have been estimated according to the OEM formalism of Rodgers (2000) on the basis of a representative subset of solar spectra.

Error source	Error (%)	Comments
Assumed variability	49.7	WACCM variability relaxed, commensurate with ACE-FTS variability down to 6 km
Systematic errors		
Line intensity HCHO	9.7	Assuming ±10 % uncertainties in HCHO line strengths
Air-broadening coefficient HCHO	8.0	Assuming ±10 % uncertainties in HCHO air-broadening coefficients
Line intensity interfering gases	5.2	Assuming the maximal HITRAN 2008 uncertainties
Instrumental line shape	2.5	±10 % misalignment and instruments bias
Forward model	1.0	Retrieval algorithm-related
HCHO a priori profile	3.0	Assuming HCHO a priori profiles derived from ACE-FTS, GEOS-Chem and IMAGES
Total systematic error	14.2	
Random errors		
Temperature profile	5.0	Assuming the NCEP profile uncertainty pattern (see text)
H_2O and HDO a priori profiles	10.1	Changes by a factor of 2 in a priori slope
SZA	0.7	Assuming ±0.1° bias
Measurement noise	14.7	
Smoothing	10.2	
Model parameters	2.1	
Total random error	21.3	

Franco et al., AMT, 2015

Uncertainty budget/Information content/vertical sensitivity

Table 3. Error budget on the retrieved HCHO vertical column density (VCD) for the MAX-DOAS measurements. The total uncertainty is calculated by adding the different error terms in Gaussian quadrature.

Error sources	Uncertainty on HCHO VCD (%)
Smoothing and noise errors	9.1
Uncertainty related to aerosols	6.3
Uncertainty related to the a priori	8.8
Uncertainty related to the albedo	1.0
Uncertainty on the HCHO cross sections	9.0
Total uncertainty	16.8

Franco et al., AMT, 2015

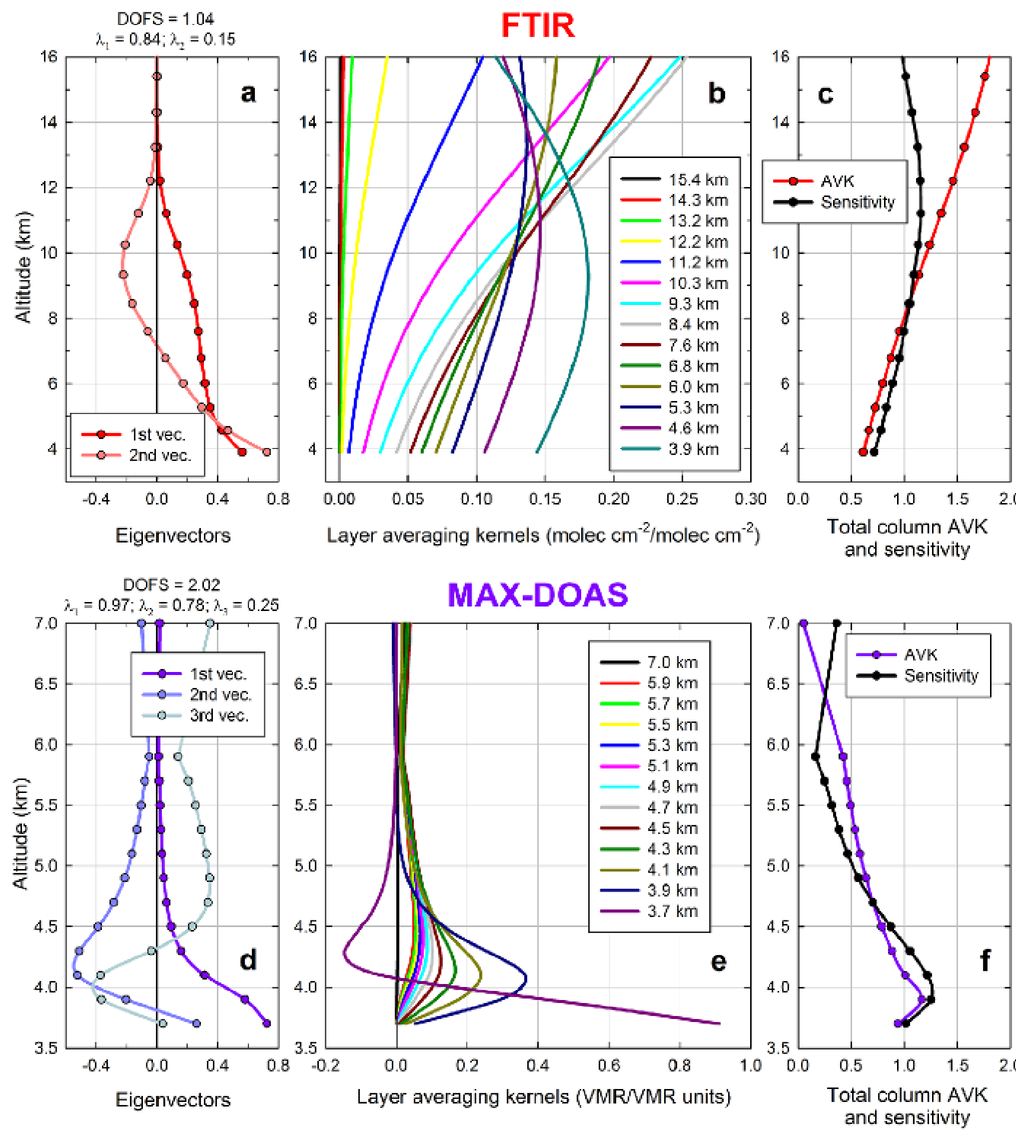

Comparison MAX-DOAS/FTIR/GEOS-Chem

Franco et al., AMT, 2015

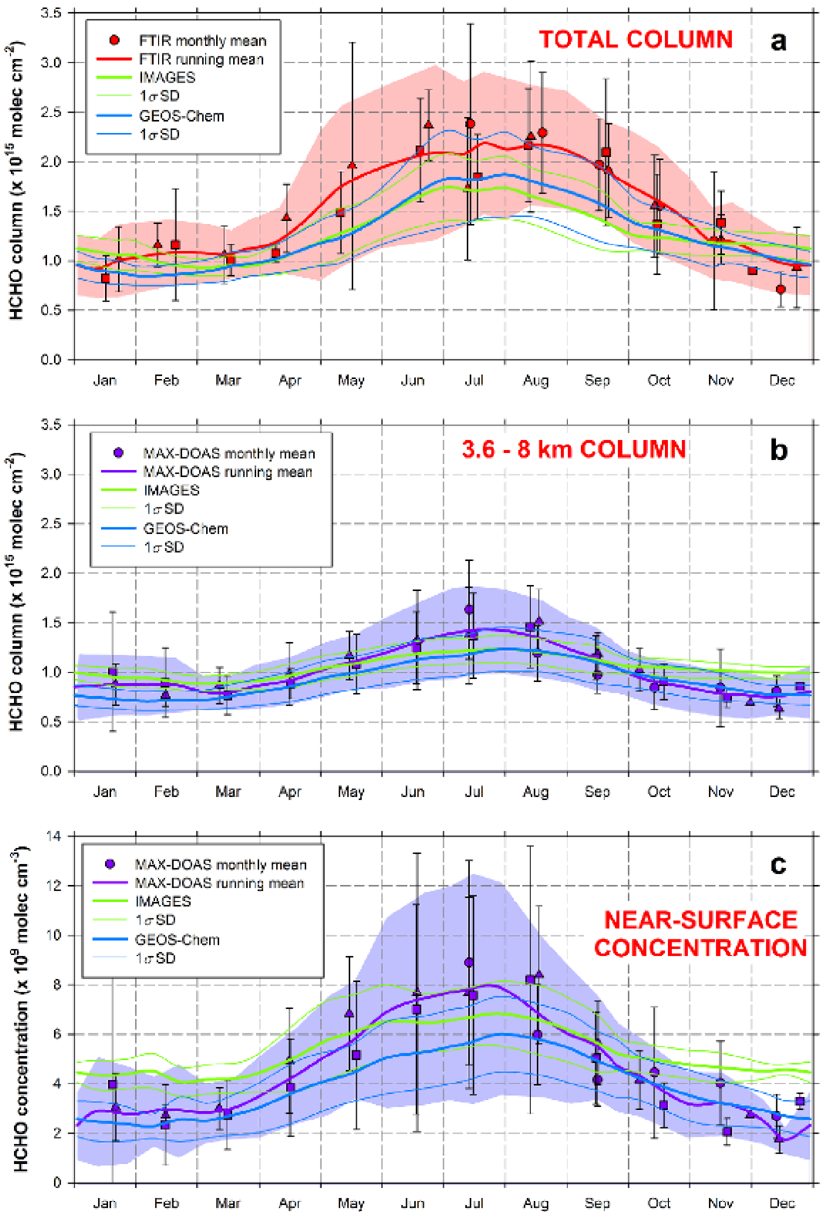

Vertical profiles

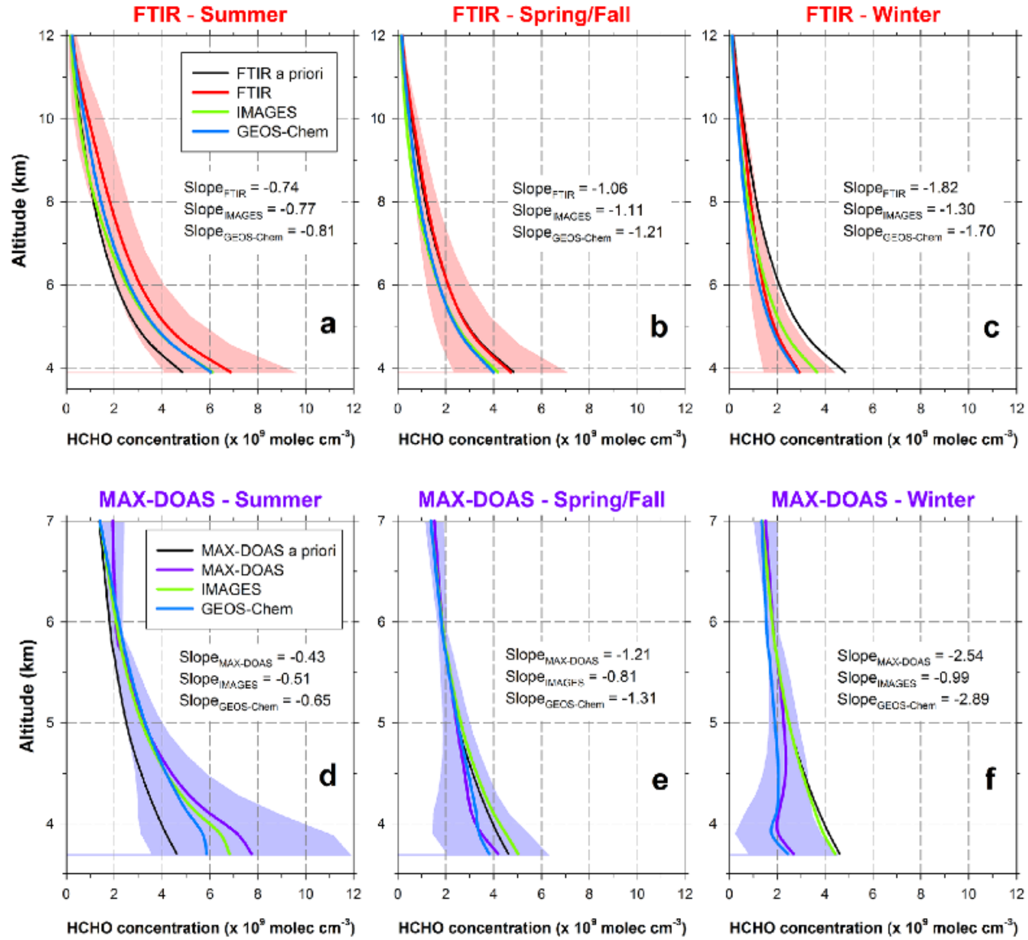

Comparisons to in situ data: MAX-DOAS

Horizontal representativeness

Gomez et al., AMT, 2013 from O_4 at 360 nm:

$$d = \frac{SCD_{O_4}(\alpha{=}0°, SZA1, t1) - SCD_{O_4}(\alpha{=}90°, SZA2, t2) f}{[O_4]_{station}}$$

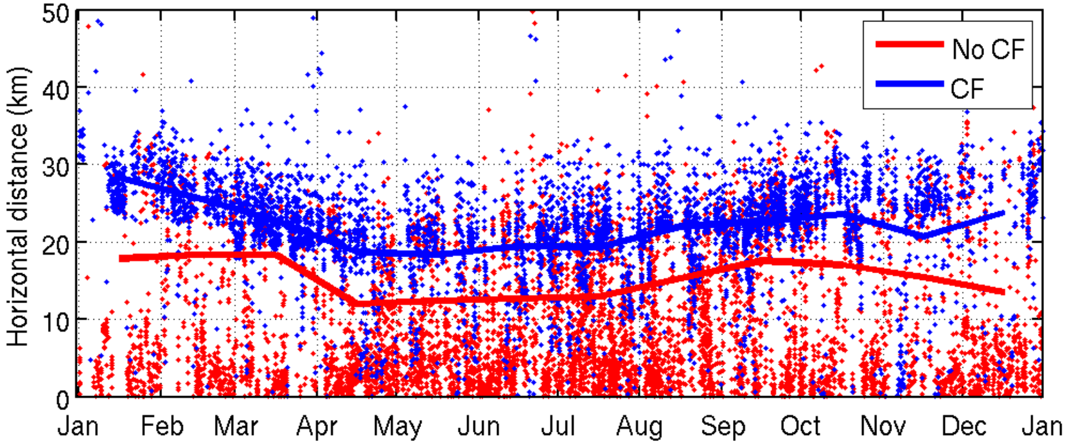

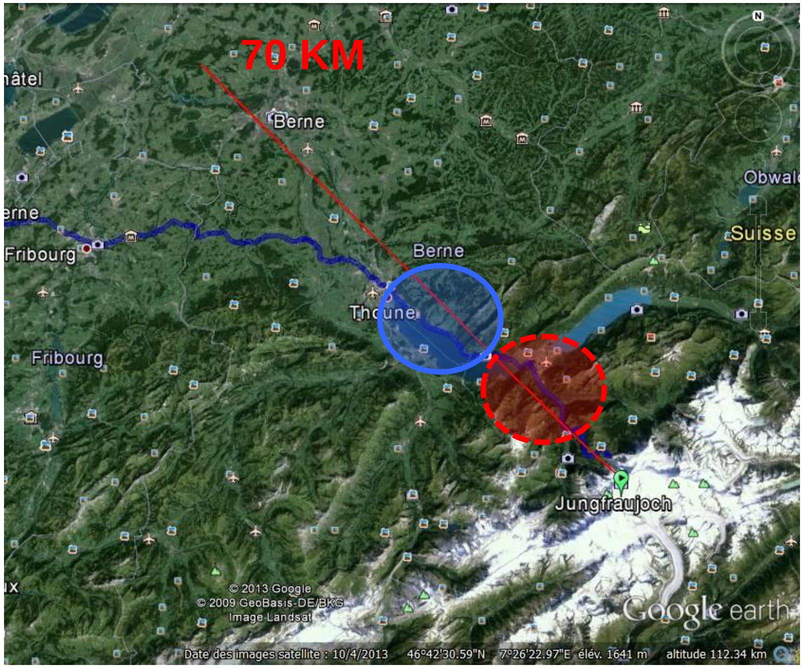

- From all scans: d~12-18km (460 nm: 25-45km)
- From cloud-filtered (only clear-sky/thin clouds) scans (CF): d~18-28 km (460 nm: 40-65km)

Near-surface NO_2 concentration

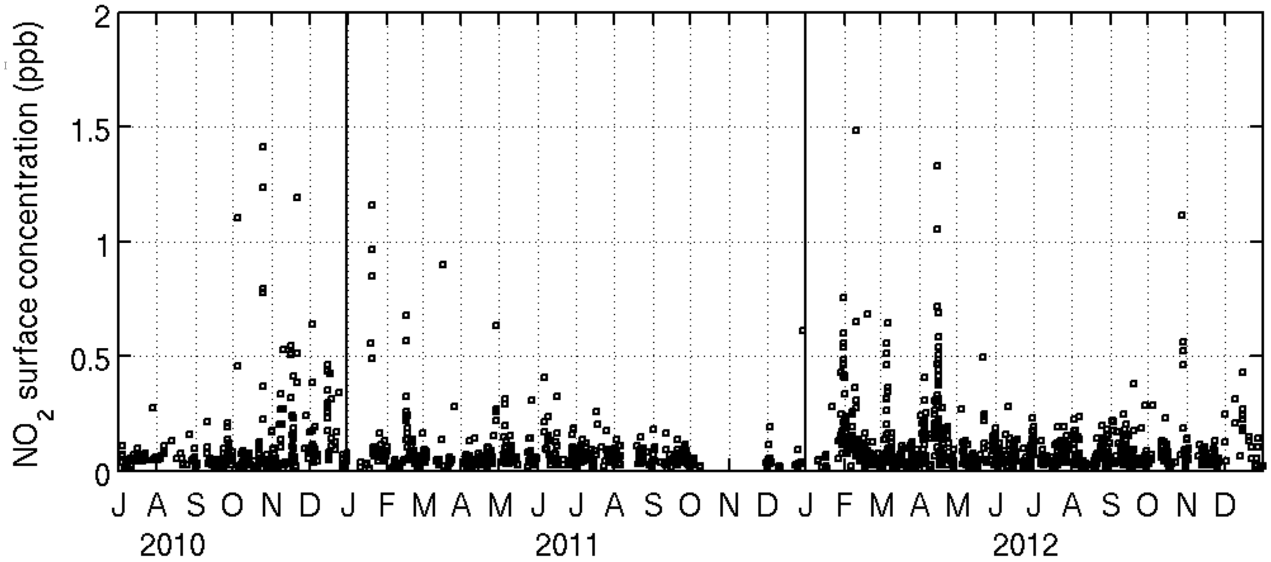

Number of useful scans: 2215

3.6-3.8km layer

Comparison with in-situ (NABEL network), R=0.69
Relatively good agreement dispite
 geographical mismatch of about 30km

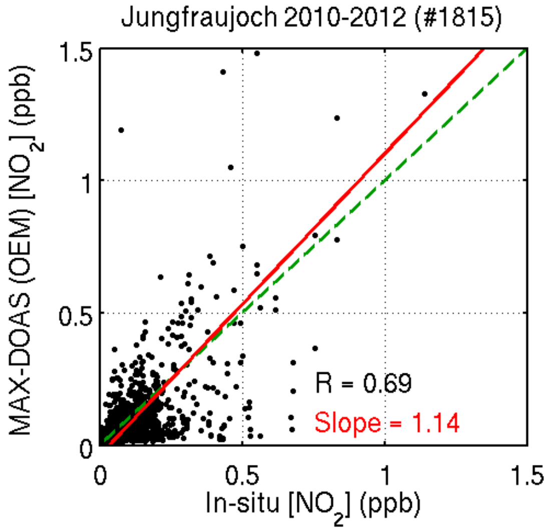

MAX-DOAS versus in-situ corrected FLEXPART

Flexpart work by S. Henne (EMPA)

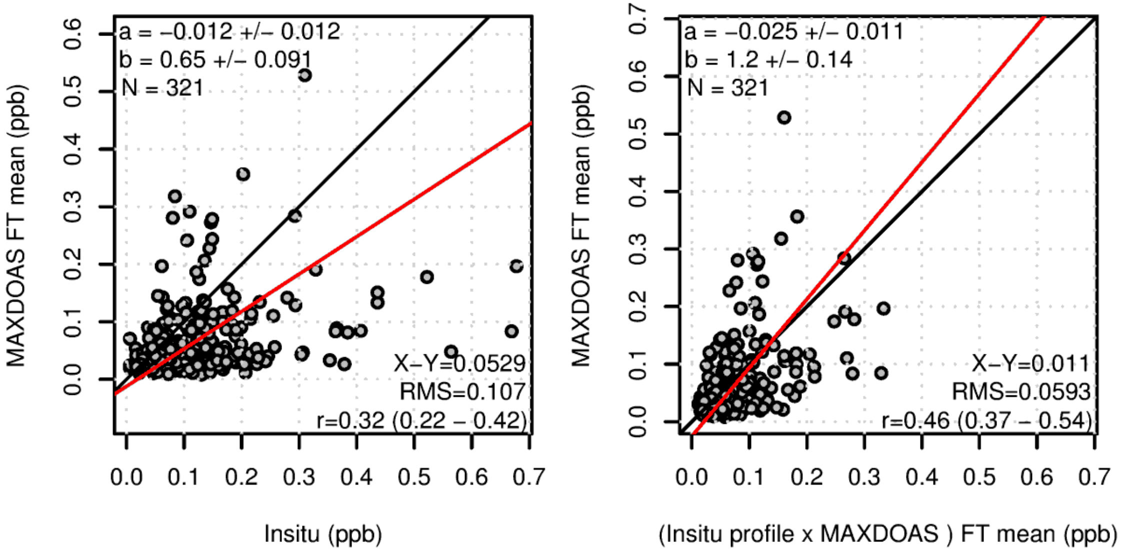

3.6-4.0km layer

In-situ-corrected FLEXPART model and also application of the MAX-DOAS averaging kernels

Slope and correlation coefficient are improved by using in situ data, but still relatively low (0.32 to 0.46)

Horizontal mismatch is a non-neglible effect

Comparisons to in situ data: FTIR

In situ vs FTIR

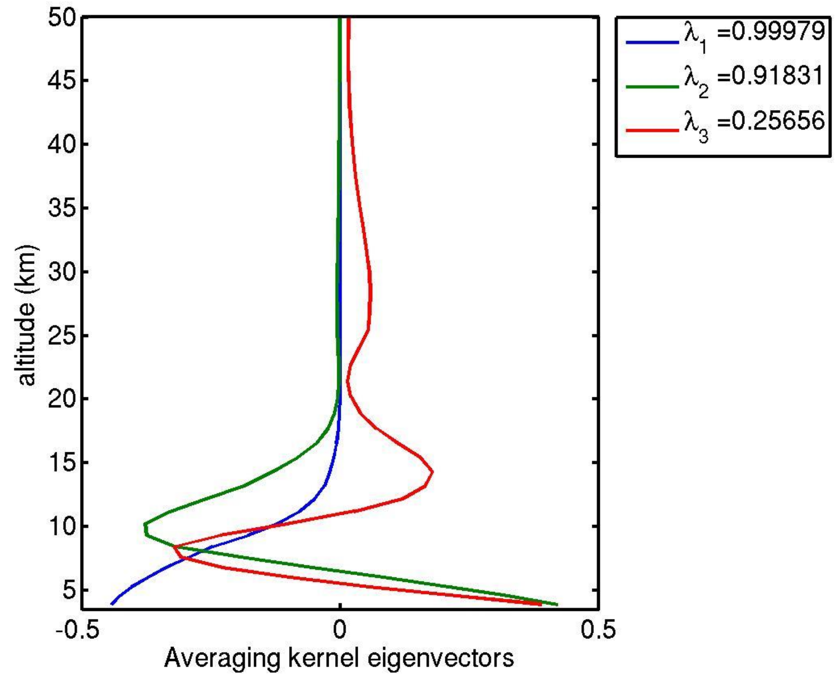

- **Great difference in sampled airmass**
  - **FTIR typically has limited profile information**
  - **~2 DOF for CH4, CO**
  - **For CO lowest partial column (DOF>1) ranges between 3.6 and 7.2 km**

The High altitude JFJ site, most of the time, represents the Free Troposphere

However on occasion, planetary boundary layer air does reach the JFJ site

The JFJ Site

De Wekker et al. Bound.-Lay. Meteo.,

113, 249-271, 2004

Aircraft to measure Aerosol layer height

Model to calculate the Convective Boundary layer height

Most of the time the AL stays below the JFJ site.

But from time to time it pushes up to 4km altitude, above the CBL

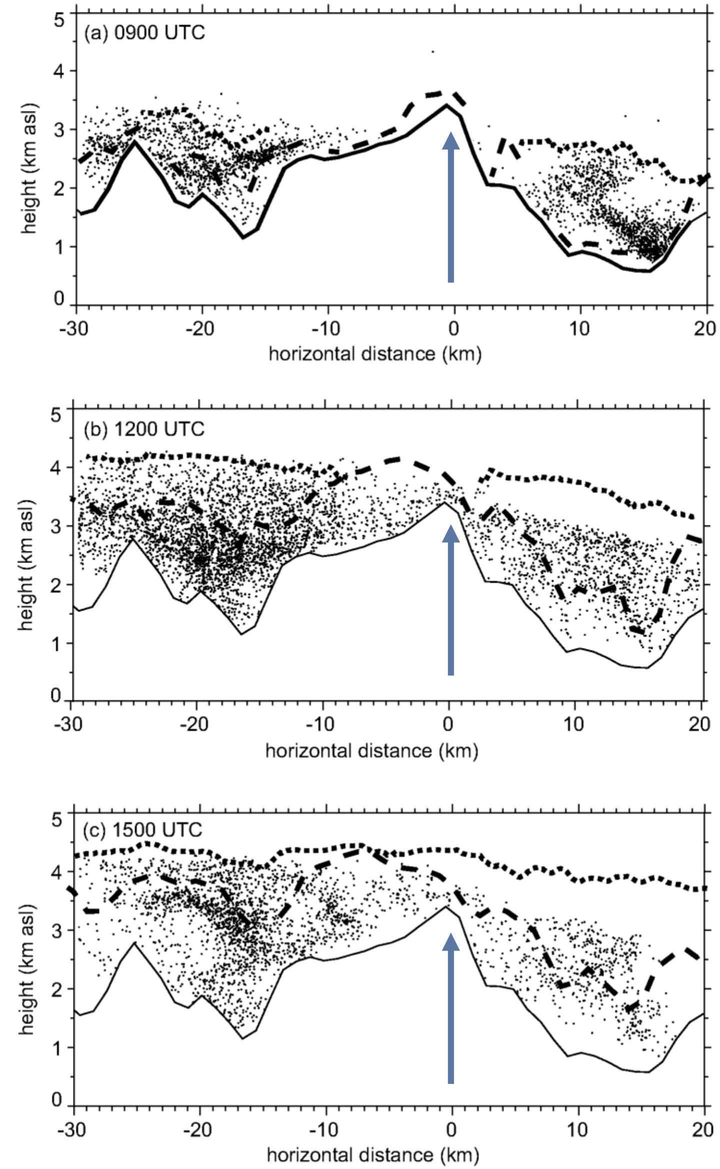

Figure 8. Cross-section of the particle distribution at 0900 UTC (a), 1200 UTC (b), and 1500 UTC (c) in a 6-km-wide band perpendicular to the mountain divide. The dotted lines in (a), (b), and (c) are observations of AL heights at 0913, 1317, and 1520 UTC from Figure 2. The dashed lines are CBL heights as determined from the model by the *Ri*-method at 0900, 1200, and 1500 UTC.

example CO

- **Strong outliers NDIR**
  - **stronger impact of boundary layer 'pollution' on the NDIR data**
  - **Impact decreases over time**

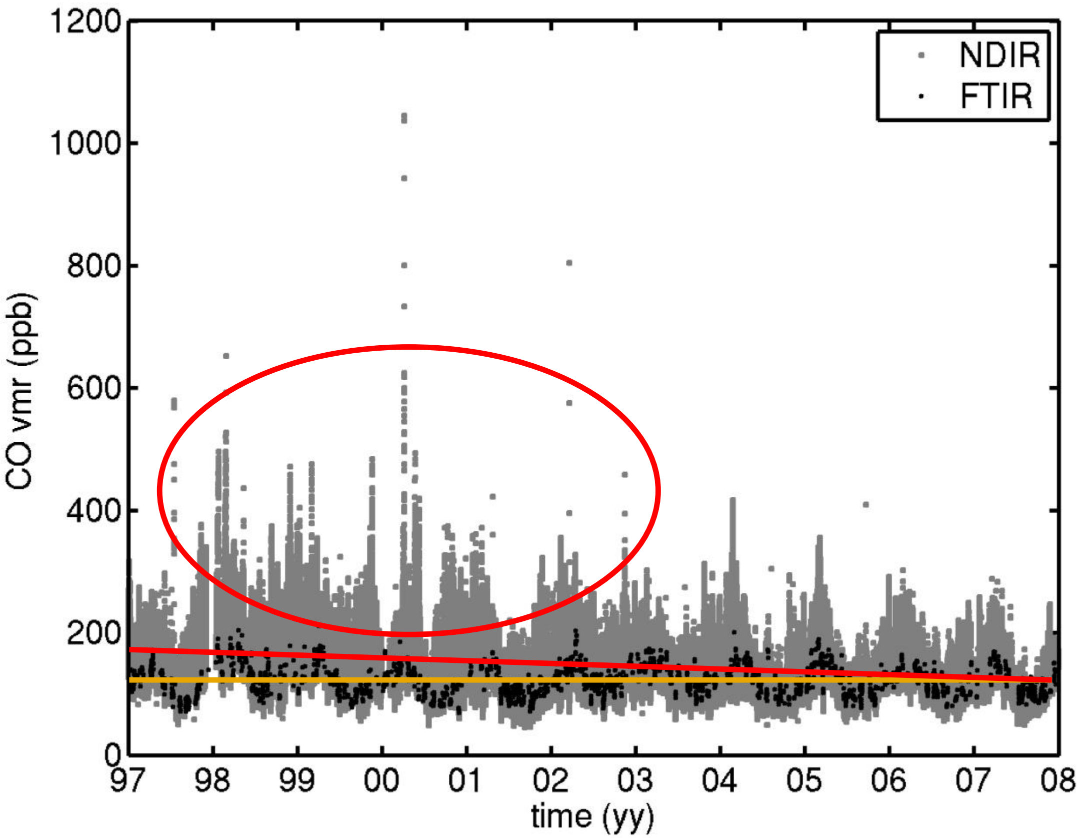

- **Different trends**
  - **NDIR: - 3.21 ± 0.03 ppb/yr**
  - **FTIR: - 0.8 ± 0.4 ppb/yr**

Background selection

- **Meteorological data:**
  - **Requires large amounts of additional data (RH, pressure gradient over the alps, wind speed, etc?) from both the JFJ and surrounding sites**
- **Trajectory analysis:**
  - **Requires accurate short time-scale trajectories. Complex orography of the alps**
- **NOy/CO ratio**
  - **Gives indication of age of airmass but no clear distinction between disturbed or undisturbed**
- **Statistical method**
  - **No additional data required**
  - **Separate Gaussian background from polluted 'tail'**

Background selection

- **Step 1: Fit function through timeseries:**
  - **Typically trendline + harmonics such as**

$$f(t) = a_1 + a_2 t + a_3 t^2 + \sum_{i=1}^{4} \left[a_{(2i+2)} \sin(2\Pi i t) + a_{(2i+3)} \cos(2\Pi i t) \right]$$

- **Step 2: Calculate the standard deviation using the negative residuals only**
- **Step 3: Remove all datapoints which have a residual value > 2 sigma**
- **Step 4: repeat step 1-3, x times**

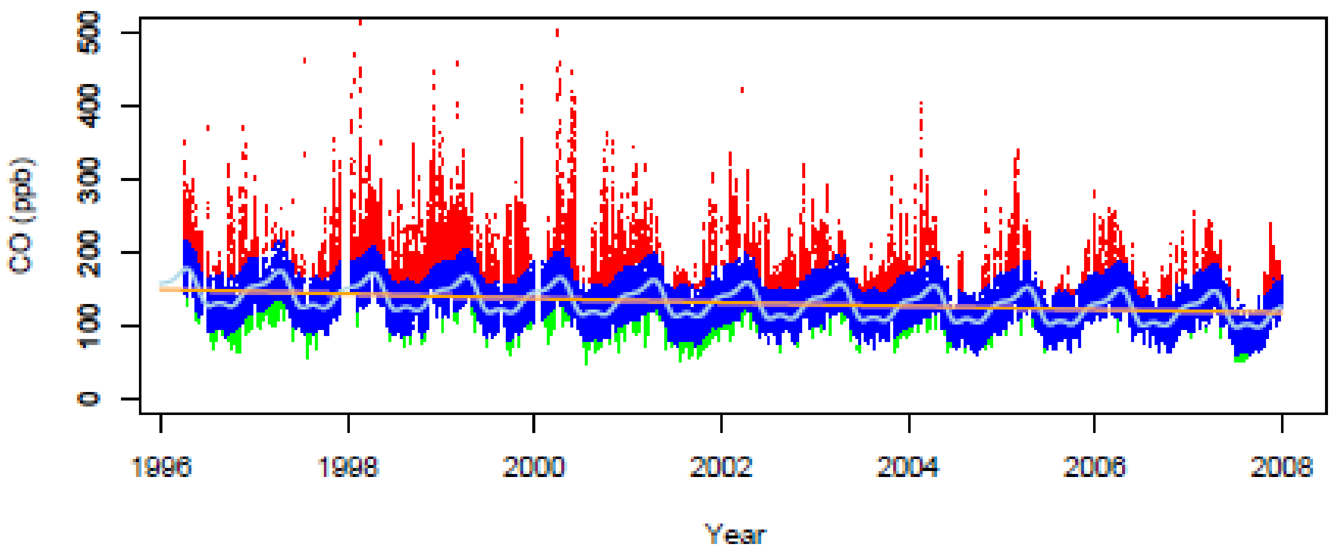

Background selection

- **Robust Extraction of Baseline Shape:**

- **Robust local regression**
    - **No presumptions on the shape o trend or seasonality**
    - **3 month window**

- **Ruckstuhl et al. Atmos. Meas. Tech. ,5,**
- **IDPmisc package, R**

- **Gives you the baseline fit only**
- **No quality marker for the individual data points**

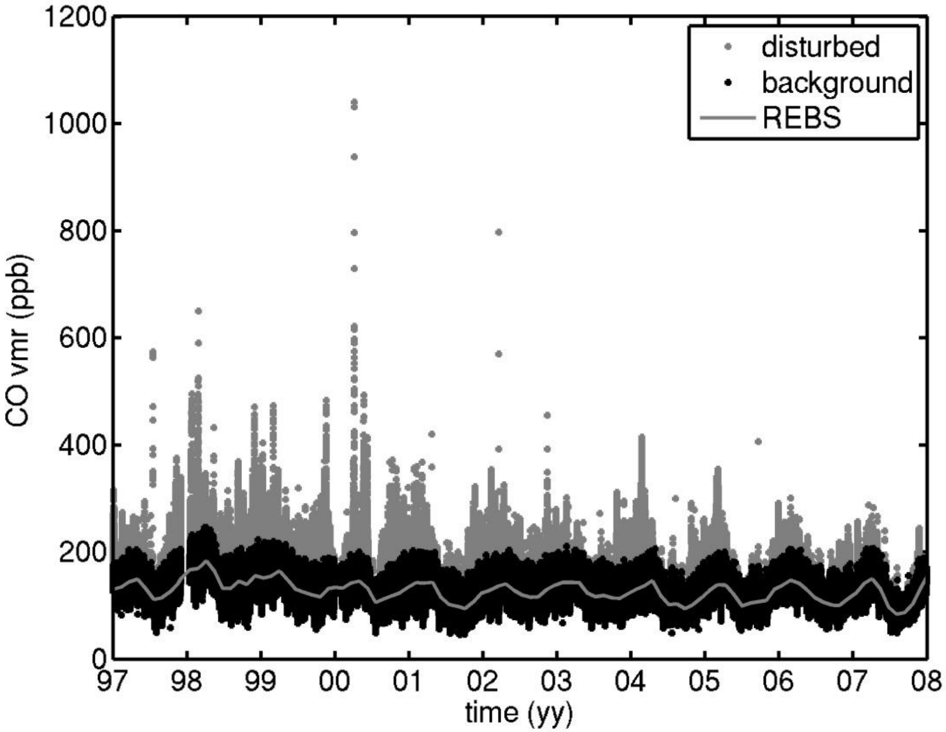

Background selection

- **Residuals (Data-baseline fit)**

- **Finds best fit for which the negative residuals have a gaussian shape**
- **All the background data should have a normal distribition**

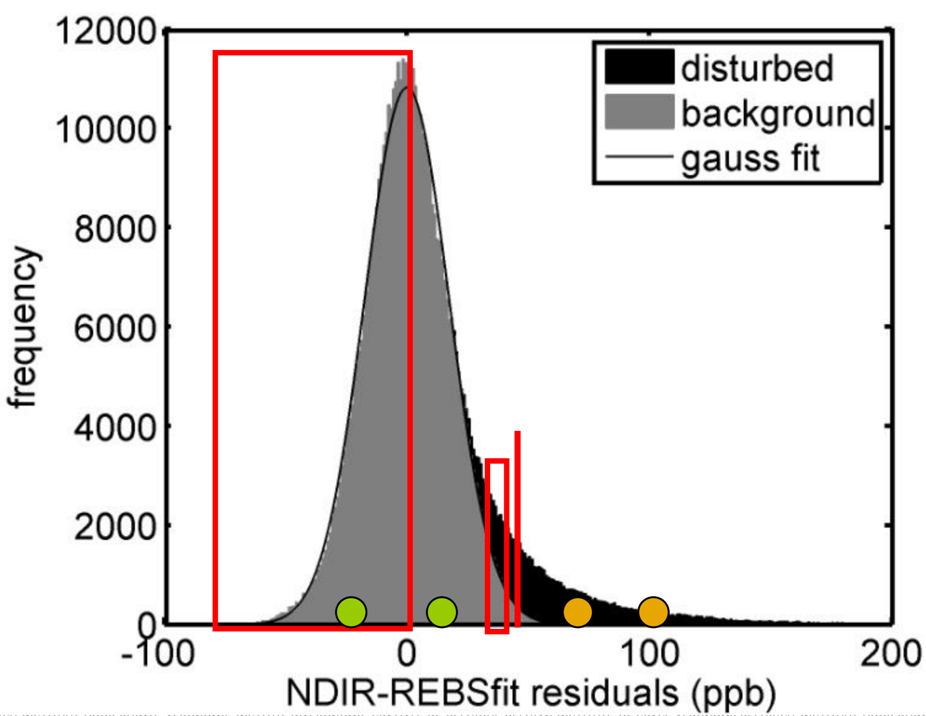

- **Reject data above the 3σ line ?**

- **Reject data in each bin (1ppb wide) with largest combined offset of its neighbouring (in time) values**

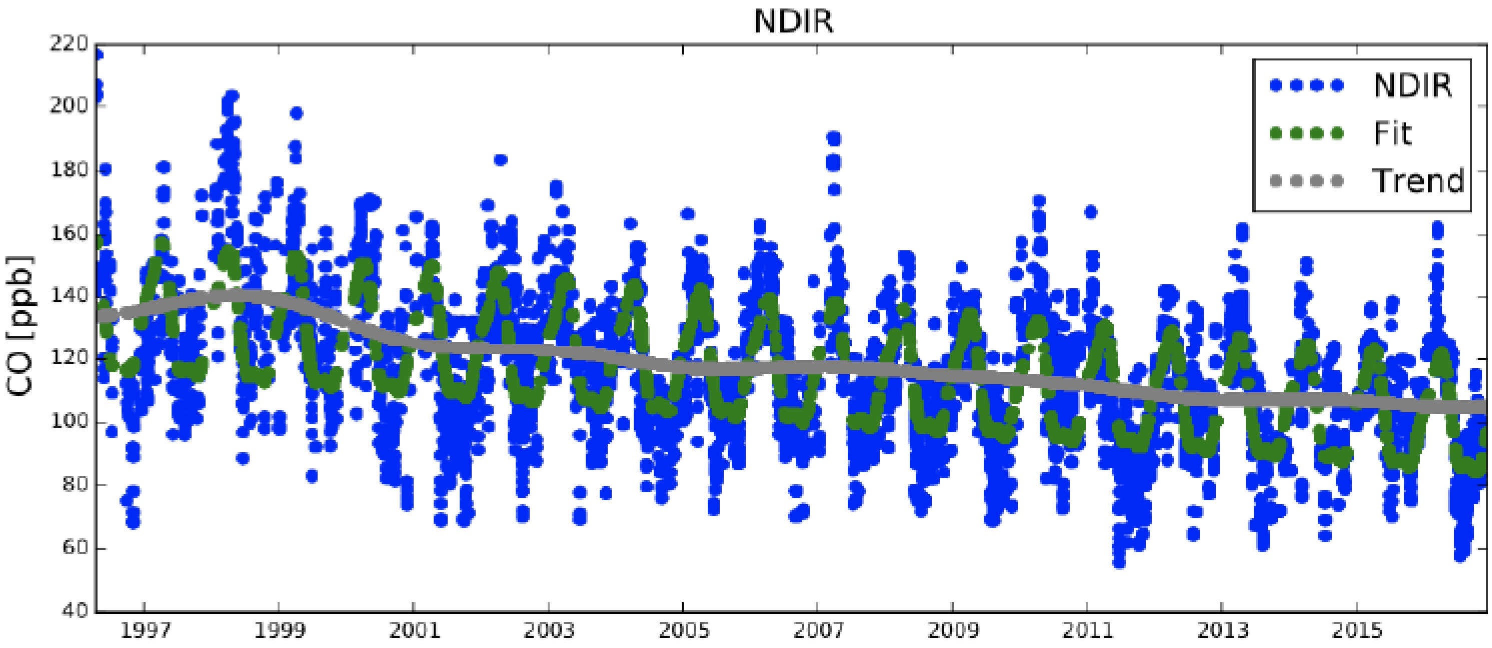
NDIR
CO [ppb]
220
200
180
160
140
120
100
80
60
40
1997
1999
2001
2003
2005
2007
2009
2011
2013
2015
NDIR
Fit
Trend

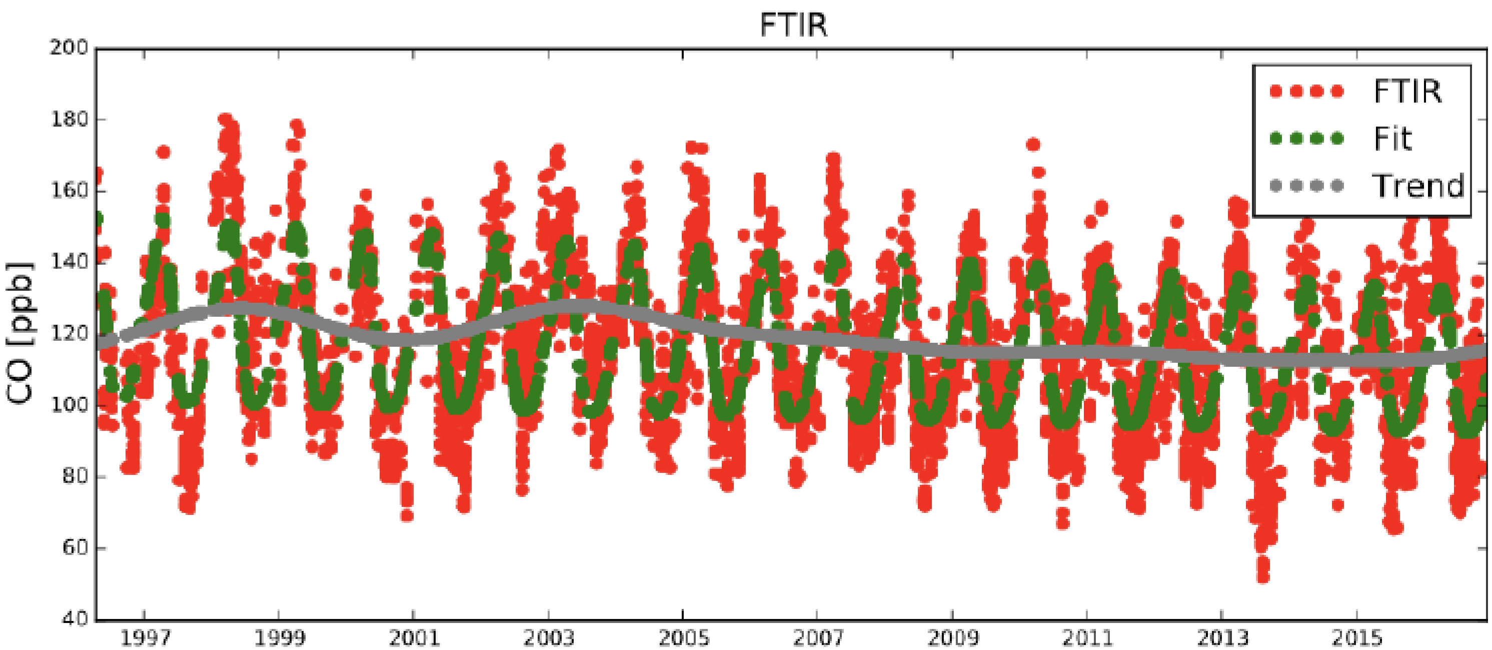
FTIR
CO [ppb]
200
180
160
140
120
100
80
60
40
1997
1999
2001
2003
2005
2007
2009
2011
2013
2015
FTIR
Fit
Trend

Very similar seasonal cycle

NDIR slightly higher in summer months
Residual PBL air?

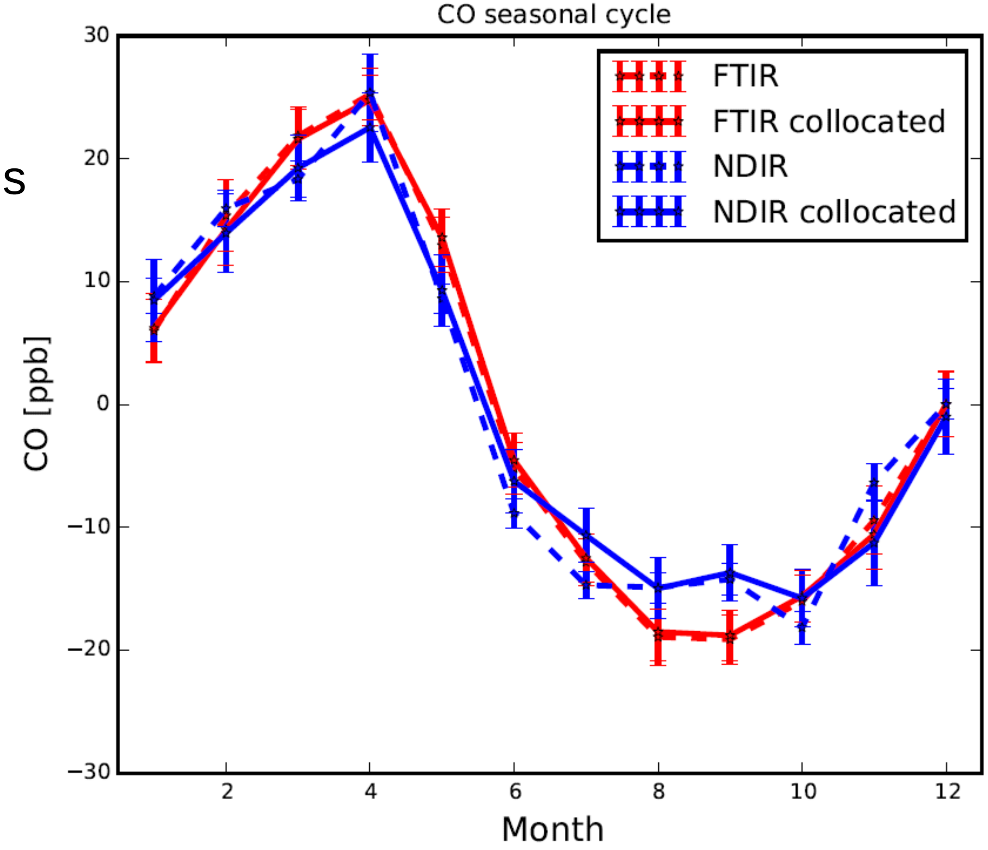

UL= all filtered
UR= no trend
BL=no seasonality
BR=no trend + seas

R UL+UR=0.77

R BL = 0.60

R BR= 0.57

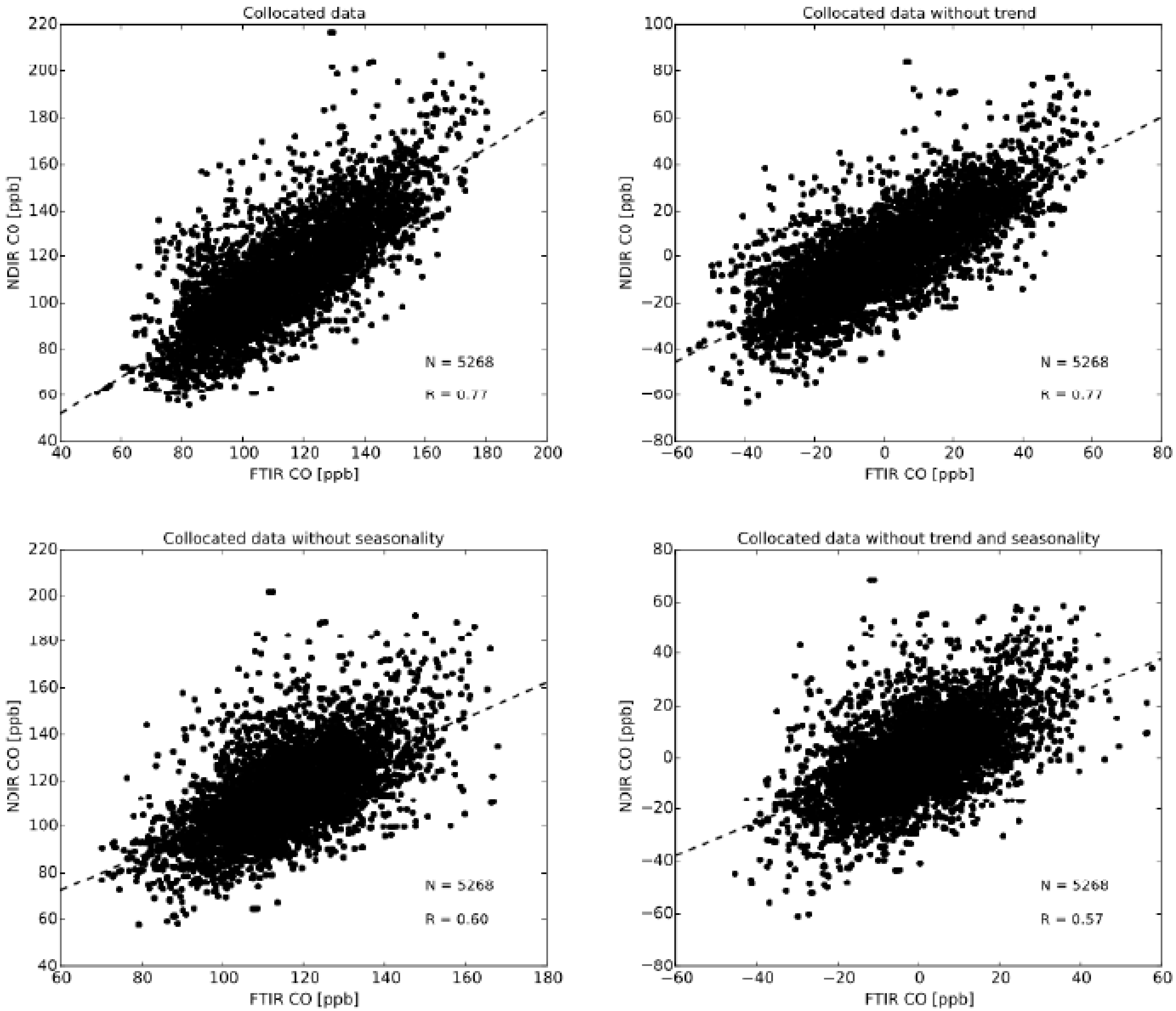

Very good results, certainly when taking into account that no smoothing correction (for instance by 'correcting' a model profile with in situ data) was used

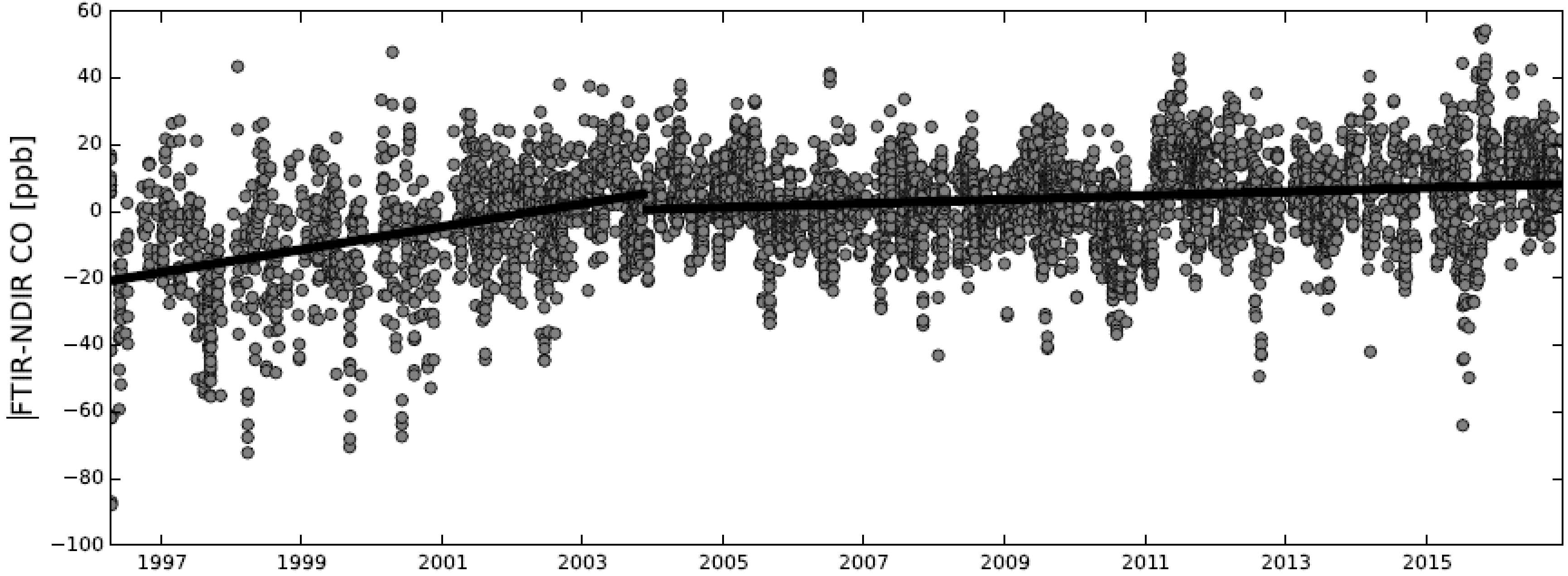

Pre 2004: Significant difference in trend??

Particularly stronger growth rate in the 2000 to 2004 FTIR growth rate

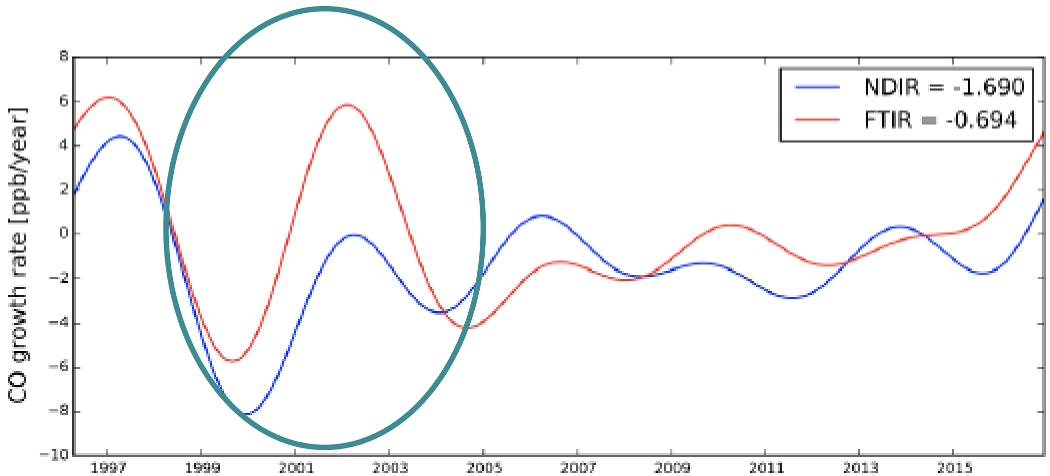

Flexpart footprint analysis:

NDIR shows much higher influence for Europe

FTIR: stronger importance of America and Asia

Paired with EDGAR and GFED emissions = simulate concentrations at the JFJ site

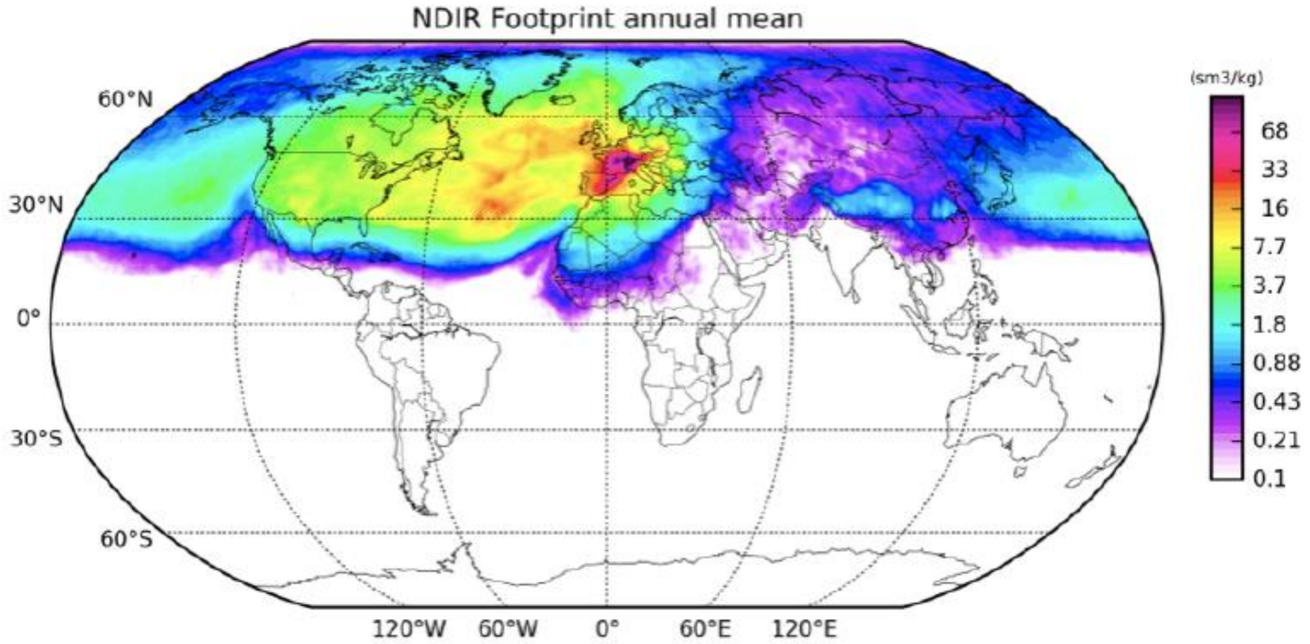

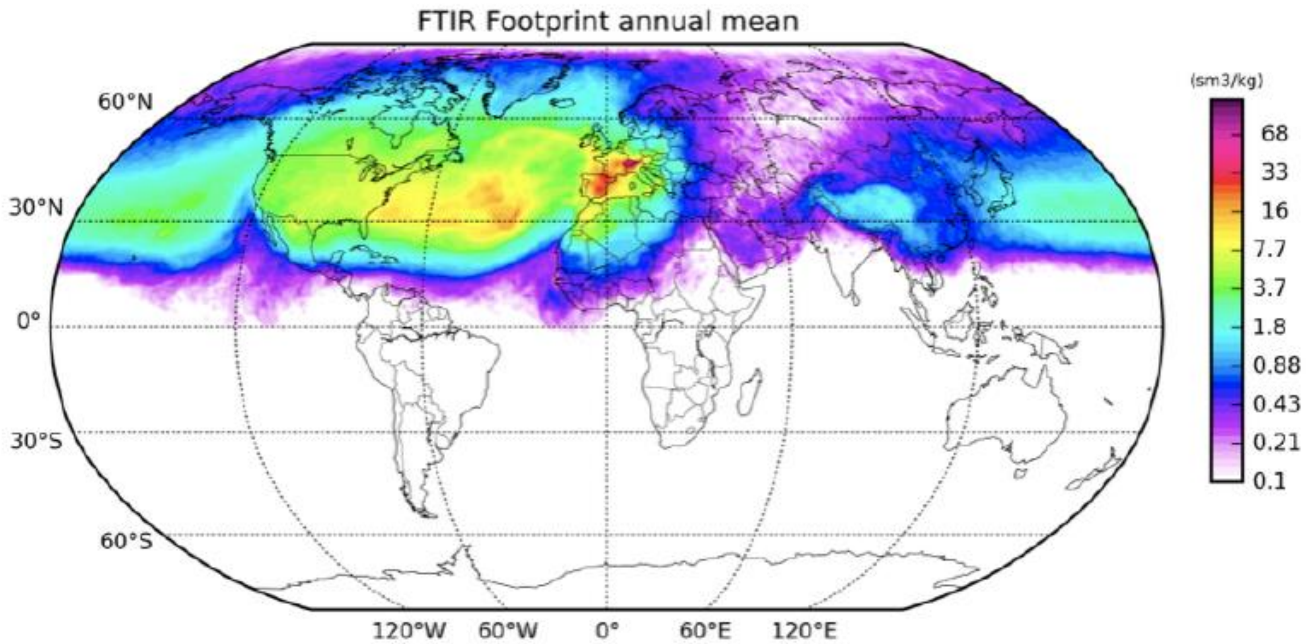

Time coverage	NDIR	FLEXPART(NDIR)	FTIR	FLEXPART(FITR)
1997-2003	-3.10±0.42	-2.71	0.69±0.78	-1.42
2004-2012	-1.09±0.37	-0.75	-0.78±0.43	-0.75
1997-2012	-1.92±0.21	-1.73	-0.73±0.27	-1.07

Tohjima, Y., Kubo, M., Minejima, C., Mukai, H., Tanimoto, H., Ganshin, A., Maksyutov, S., Katsumata, K., Machida, T., and Kita, K.: Temporal changes in the emissions of CH4 and CO from China estimated from CH4/CO2 and CO/CO2 correlations observed at Hateruma Island, Atmos. Chem. Phys., doi:10.5194/acp-14-1663-2014, 2014.

Tohjima et al. (2014) used the observations at Hateruma Island to estimate the CO emission from China. They found that the CO emission from China is increasing before 2004 and starts to decrease after 2004, while the CO emission from the EDGAR v4.2 shows the CO emission is almost constant before 2001 and keeps increasing after 2001. Apart from that, the CO emission from the EDGAR v4.2 is much lower than their study and also other inventories.

→ Consistent with our observed growth rates

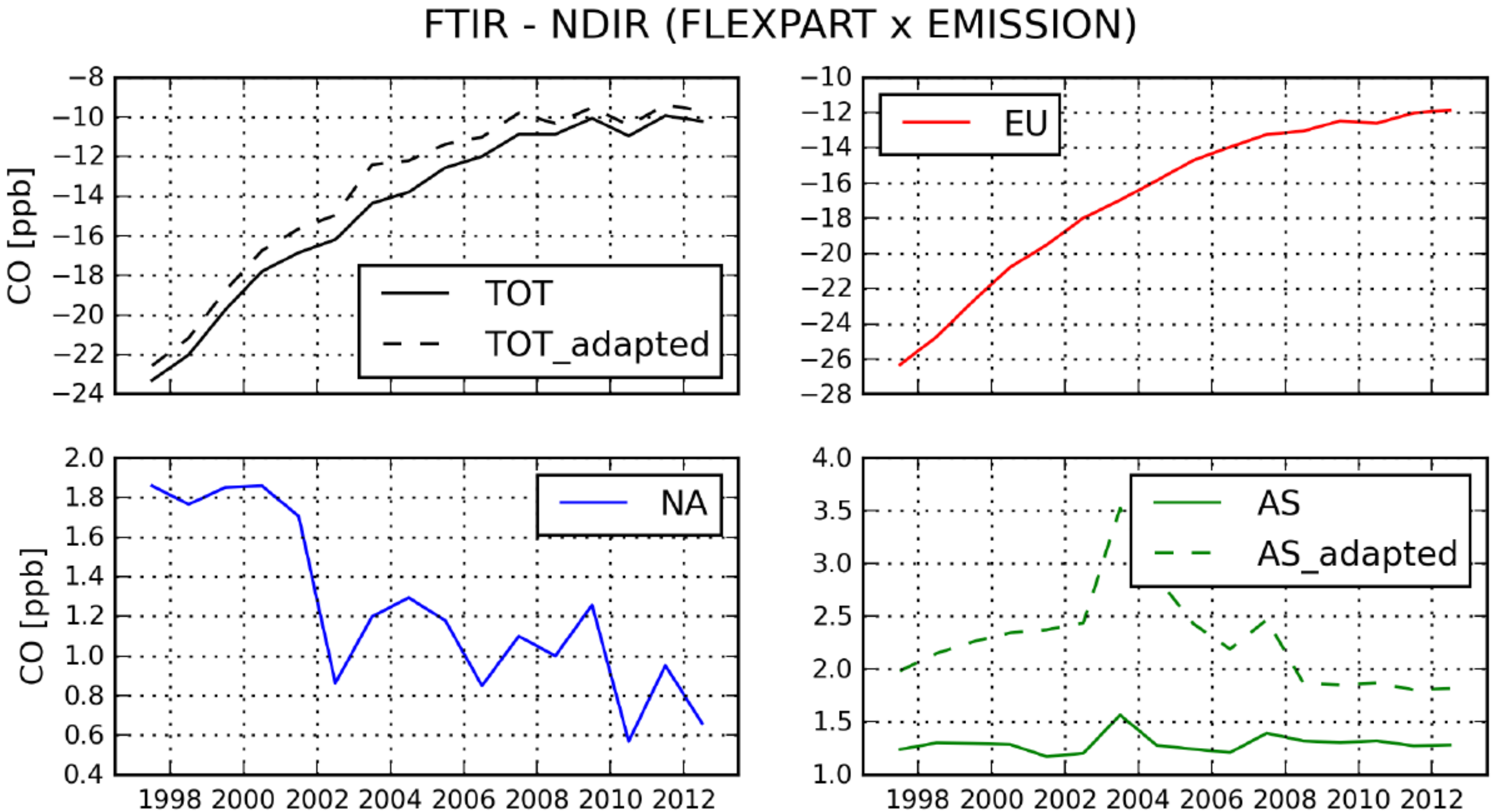

Improvement with Tohjima but impact does not cover 100% our observations

- Even bigger influence of Asian emissions?
- 20 day back trajectory not sufficient in time?
- Asian emission peak still underestimated?

Conclusions

- **Direct comparisons between ground-based in situ and remote sensing is not straightforward**

- **Critical selection of data and using models as a go-between (even between 2 remote sensing techniques) is often required**

- **Nevertheless, comparisons often still produce very useful scientific results**